



Cite this: DOI: 10.1039/c8nj00797g

# New Pd/Pt(II) complexes as unsymmetrical ylide-based chemotherapeutic agents: synthesis, characterization, biological activity, electrochemical, and X-ray studies†

Seyyed Javad Sabounchei,<sup>a</sup> Khadijeh Badpa,<sup>a</sup> Davood Nematollahi,<sup>a</sup> Mahnaz Sharafi-kolkeshvandi,<sup>a</sup> Leila Hosseinzadeh,<sup>b</sup> Roya Karamian,<sup>c</sup> Fatemeh Ghasemlou<sup>c</sup> and Robert W. Gable<sup>d</sup>

New Pd/Pt-complexes were synthesized by incorporating  $\alpha$ -keto stabilized unsymmetrical phosphorus ylides  $[\text{Ph}_2\text{P}(\text{CH}_2)_n\text{PPh}_2=\text{C}(\text{H})\text{C}(\text{O})\text{C}_6\text{H}_4\text{-}p\text{-Ph}]$  ( $n = 1$ , (**Y**<sup>1</sup>);  $n = 2$ , (**Y**<sup>2</sup>)) and  $\text{M}(\text{Cod})\text{Br}_2$  ( $\text{M} = \text{Pt}, \text{Pd}$ ;  $\text{Cod} = 1,5\text{-cyclooctadiene}$ ). The obtained P,C-chelated  $[\text{PdBr}_2(\kappa^2\text{-Y}^1)]$  (**1**),  $[\text{PtBr}_2(\kappa^2\text{-Y}^1)]$  (**2**),  $[\text{PdBr}_2(\kappa^2\text{-Y}^2)]$  (**3**), and  $[\text{PtBr}_2(\kappa^2\text{-Y}^2)]$  (**4**) complexes were characterized successfully by FT-IR and NMR (<sup>1</sup>H, <sup>13</sup>C, and <sup>31</sup>P) spectroscopic methods. The structures of **1**, **2**, and **3** were elucidated by single crystal X-ray structural analyses. The structures of **1** and **2** consist of five-membered rings, while that of **3** has a six-membered ring, formed by coordination of the ligand with the phosphine group and the ylidic carbon atom to the metal center. Moreover, the cytotoxic effects of the compounds were studied by a MTT assay in three human carcinoma cell lines: A2780, H1299, and U87 MG. The compounds proved to be outstanding potent cytotoxic agents against the A2780 cell line and can be considered as a promising lead in cancer-treating drug discovery and development. Also, these newly synthesized compounds were evaluated for their *in vitro* antioxidant and antifungal activities by using 2,2-diphenyl-1-picrylhydrazyl (DPPH) free radical-scavenging and potato dextrose agar (PDA) medium, respectively. The results showed that these compounds exhibited excellent biological activities.

Received 16th February 2018,  
Accepted 8th April 2018

DOI: 10.1039/c8nj00797g

rsc.li/njc

## Introduction

Previous studies on anti-tumor activity with cisplatin began in the mid-1970s (Fig. S1, ESI†), followed by proving its considerable activity against sarcoma 180 and leukemia L1210 tumors in mice.<sup>1</sup> However, the *trans*-isomer (Fig. S1, ESI†) of this complex cannot form particular intra-strand adducts due to a stereochemical restriction. Furthermore, biologically processing of these adducts is more complex than that of *cis*-isomer.<sup>1</sup>

Although cisplatin is now applied in treating a wide range of cancers, including that of testicular, ovarian, bladder, head and

neck, lung, and cervix,<sup>1</sup> it still has some problems including the following: (A) most of cancers resist the treatment with cisplatin<sup>2</sup> and (B) cisplatin causes many side-effects.<sup>1,2</sup> Nevertheless, cisplatin, as a platinum-based anticancer drug, has raised interests in the development of new generation of platinum-based anticancer agents.<sup>3–8</sup> Useful cisplatin analogues are carboplatin and oxaliplatin.<sup>9–12</sup> Although the inherent dark toxicity and cellular resistivity of cisplatin have yet created challenges,<sup>13–17</sup> such toxic side effects have been reduced when carboplatin is used (Fig. S2, ESI†) owing to its much lower reactivity. Oxaliplatin (Fig. S2, ESI†) has also been demonstrated to be effective for using orally in treating some cisplatin-resisted cancer like colorectal cancer.<sup>18–23</sup>

Recently, some strategies have been developed to synthesize metal-based anticancer drugs. One strategy is changing the nitrogen coordinated ligand, which is responsible for the structure of the adducts formed upon interacting with DNA or changing the halide leaving group that affects intracellular distribution of the platinum complexes and improves the toxicity profile of the drug. Another strategy has focused on applying the Pt(IV) complexes or changing the type of metal center (*e.g.* Pd(II) complexes).<sup>24–26</sup> Studies have shown that the complex compounds of both Pd<sup>2+</sup> and Pt<sup>2+</sup> ions are effective in

<sup>a</sup> Faculty of Chemistry, Bu-Ali Sina University, Hamedan, 65174, Iran.

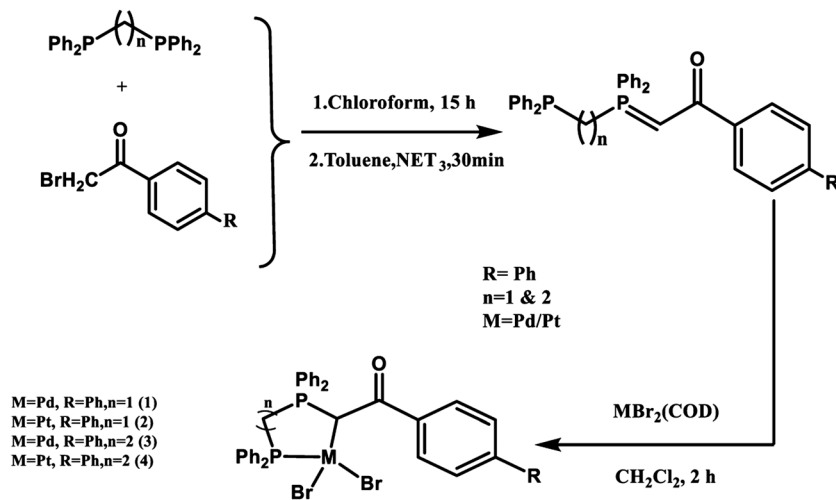
E-mail: jsabounchei@yahoo.co.uk; Fax: +988138273231; Tel: +98 8138272072

<sup>b</sup> Pharmaceutical Sciences Research Center, Kermanshah University of Medical Sciences, Kermanshah, Iran

<sup>c</sup> Department of Biology, Faculty of Science, Bu-Ali Sina University, P. O. Box 65175/4161, Hamedan, Iran

<sup>d</sup> School of Chemistry, University of Melbourne, Victoria, 3010, Australia

† Electronic supplementary information (ESI) available: Physical measurements and selected <sup>31</sup>P, <sup>13</sup>C, and <sup>1</sup>H NMR spectra of some compounds can be found in the online version. CCDC 1559667, 1576663 and 1576674 for the complexes 1–3. For ESI and crystallographic data in CIF or other electronic format see DOI: 10.1039/c8nj00797g



Scheme 1 Synthesis of complexes 1–4.

cell apoptosis; however, the compounds of platinum(II) have shown more potent activity.<sup>27</sup> The ligand exchange kinetics is a key factor that might explain why the platinum compounds are the most useful. The hydrolysis occurring in the palladium complexes is  $10^5$  faster than that in the corresponding platinum analogues. This feature causes the former to change into very reactive species that would not reach the pharmacological targets.<sup>28–32</sup> Thus, taking into account the high reactivity of the palladium(II) complexes, to develop anticancer drugs based on palladium(II), these complexes need to be stabilized to some extent through strong coordination with a nitrogen ligand and a suitable leaving group. Due to the non-lability of these groups, the drug can preserve its structure for a long time. Recently, the biological mechanism of the palladium(II) complexes with an emphasis on the cyclopalladated complexes has been investigated.<sup>33</sup> Moreover, some unsymmetrical  $\alpha$ -keto stabilized phosphorus ylides were synthesized by our group. These ylides were coordinated to various transition metal ions such as Hg(II), Ag(I), Cu(I), Pd(II), and Pt(II).<sup>34,35</sup> In this study, we selected the ylides  $[\text{Ph}_2\text{P}(\text{CH}_2)_n\text{PPh}_2=\text{C}(\text{H})\text{C}(\text{O})\text{C}_6\text{H}_4\text{-}p\text{-Ph}]$  ( $n = 1$ , ( $\text{Y}^1$ );  $n = 2$ , ( $\text{Y}^2$ )) to participate as ligands for preparations of some cyclometal complexes (Scheme 1). Furthermore, we reported the synthesis, characterization, and application of new Pd/Pt-bromo complexes 1–4 containing stabilized phosphorus ylides towards the anticancer, antioxidant, and antifungal activities.

## Result and discussion

### Synthesis

Dppe or dppm was reacted with 1 equiv. of 2-bromo-4'-phenylacetophenone to form the corresponding diphosphonium salts. Further treatment of these salts with triethyl amine led to the elimination of HBr, affording the unsymmetrical diphosphine ylides in 80–85% yield. The reaction of these ligands with  $[\text{Pd/PtBr}_2(\text{Cod})]$  in an equimolar ratio yielded new P,C-chelated metalla-complexes  $[\text{MBr}_2(\text{Ph}_2\text{P}(\text{CH}_2)_n\text{PPh}_2\text{C}(\text{H})\text{C}(\text{O})\text{C}_6\text{H}_4\text{-}p\text{-Ph})]$  ( $n = 1$ ,  $\text{M} = \text{Pd}$  (1);  $n = 1$ ,  $\text{M} = \text{Pt}$  (2);  $n = 2$ ,  $\text{M} = \text{Pd}$  (3); and  $n = 2$ ,

$\text{M} = \text{Pt}$  (4)) in 80–90% yield (Scheme 1). All complexes are soluble in chloroform and dichloromethane and insoluble in non-polar solvents, such as *n*-hexane and petroleum ether.

### Spectroscopy

The structure of the products was characterized successfully by  $^1\text{H}$ ,  $^{13}\text{C}$ ,  $^{31}\text{P}$  NMR, and IR spectroscopic methods. Table 1 shows the brief summary of the collected data ( $^1\text{H}$ ,  $^{13}\text{C}$ ,  $^{31}\text{P}$  NMR, and IR). Moreover, the structures of the complexes 1, 2, and 3 were unequivocally determined by single crystal X-ray structural analyses.

### Infra-red spectra

As noted in the literature,<sup>36</sup> coordination of the phosphorus ylides through carbon (chelating mode) causes a significant increase in the  $\nu(\text{CO})$  frequency. The  $\nu(\text{CO})$  in the IR spectra of phosphorus ylides  $\text{Y}^1$  and  $\text{Y}^2$  were observed at lower frequencies than those of the related phosphonium salts. In the IR spectra of complexes 1–4,  $\nu(\text{CO})$  showed a significant frequency shift compared to those of the related phosphorus ylides  $\text{Y}^1$  and  $\text{Y}^2$ . These observations suggested the chelation of ylides through the P and C $\alpha$  atoms. The presence of the  $\nu(\text{CO})$  bands at around  $1600\text{ cm}^{-1}$  in the IR spectra of these complexes indicated that the products (*i.e.*, P,C-chelated complexes) were formed. Furthermore, the IR spectra of complexes 1–4 did not show the  $\nu(\text{CO})$  bands at around  $1500\text{ cm}^{-1}$ , confirming that no significant amount of P,P-coordinated complexes as side products were formed.

### NMR spectral data

The  $^{31}\text{P}$  NMR chemical shift values for all complexes shifted downfield with respect to all parent ylides, indicating that the coordination of the ylides has occurred. The coordination of phosphorus ylides in the P,C-chelated form created a large chemical shift for both (PPh<sub>2</sub>) and (PCH) phosphorus groups. The  $^{31}\text{P}$  NMR spectrum of complex 1 shows two doublet peaks at around  $\delta = 26.2$  and  $38.4$  ppm, which is assigned to PPh<sub>2</sub> ( $\text{P}_a$ )

Table 1 Spectroscopic data for compounds **Y**<sup>1</sup>, **Y**<sup>2</sup>, and **1–4**

Compound	IR; $\nu(\text{CO})$ ( $\text{cm}^{-1}$ )	<sup>1</sup> H NMR; $\delta(\text{PCH})$ (ppm)	<sup>13</sup> C NMR; $\delta(\text{CO})$ (ppm)	<sup>31</sup> P NMR; $\delta(\text{PCH})$ and (PPh <sub>2</sub> ) (ppm)
<b>Y</b> <sup>1</sup>	1568	4.4	185.2	15.3, -29.5
<b>1</b>	1601	6.3	196.2	38.4, 26.2
<b>2</b>	1600	5.8	195.6	42.4, 5.9
<b>Y</b> <sup>2</sup>	1565	4.3	186.8	17.1, -12.8
<b>3</b>	1600	6.4	196.2	28.7, 23.8
<b>4</b>	1600	6.5	195.9	20.1, 6.6

and PCH (**P<sub>b</sub>**), respectively (Fig. 1). The <sup>31</sup>P NMR spectrum of complex **2** shows two doublet peaks at around  $\delta = 5.9$  along with two satellite peaks due to <sup>195</sup>Pt–<sup>31</sup>P coupling and 42.4 ppm, which is assigned to PPh<sub>2</sub> (**P<sub>a</sub>**) and PCH (**P<sub>b</sub>**), respectively (Fig. 1). The <sup>31</sup>P NMR spectrum of complex **3** shows two doublet peaks at around  $\delta = 23.8$  and 28.7 ppm, which is assigned to PPh<sub>2</sub> (**P<sub>a</sub>**) and PCH (**P<sub>b</sub>**), respectively (Fig. 1). The <sup>31</sup>P NMR spectrum of complex **4** shows a different pattern with two doublet peaks around  $\delta = 6.6$  and 20.1 ppm (along with two satellite peaks due to <sup>195</sup>Pt–<sup>31</sup>P coupling), which is assigned to PPh<sub>2</sub> (**P<sub>a</sub>**) and PCH (**P<sub>b</sub>**), respectively (Fig. 1).

The <sup>1</sup>H NMR spectra of P,C-chelated complexes **1–4** exhibit the characteristic shifts of the methinic proton signals. This is interesting because the complexation of the ylides (**Y**<sup>1</sup>/**Y**<sup>2</sup>) with Pd/Pt through a free phosphorus atom did not significantly change the chemical shift values of <sup>1</sup>H NMR signals. However, the coordination through carbanion caused the PCH peaks to shift to higher frequency of around 5.8–6.5 ppm. The <sup>1</sup>H NMR spectra of complexes **1–4** show the signal of the methinic proton as a broad peak at around 6 ppm due to the coupling with neighbor phosphorus atoms. The <sup>1</sup>H chemical shift values for these complexes shifted downfield with respect to the parent ylides, also indicating that the coordination of the ylide through P and C $\alpha$  atoms has occurred.

The <sup>13</sup>C NMR spectra of complexes **1** and **2** show a downfield shift of the signals of CO, PCH, and PCH<sub>2</sub> groups with respect to the parent ylide **Y**<sup>1</sup>. The chemical shift values in the <sup>13</sup>C NMR spectra of complexes **3** and **4** show a significant shift in comparison with those of the parent ylide **Y**<sup>2</sup>. This observation also confirmed that the coordination of ylides **Y**<sup>1</sup> and **Y**<sup>2</sup> occurred through the P and C coordination sites.

### Crystallography

Suitable single crystals of complexes **1**, **2**, and **3** were grown by slow evaporation of their dichloromethane solution. The molecular structures of **1**, **2**, and **3** are shown in Fig. 2 and 3. Relevant parameters concerning data collection and refinement are given in Table 2, while selected bond distances and angles are displayed in Table 3.

Compound **1** and **2** are isostructural. In both compounds, the metal atom is in a slightly distorted square-planar environment and coordinated by two bromine atoms, one phosphorus atom, and one ylidic carbon atom. The four coordinating atoms show a slight tetrahedral distortion with a RMS deviation of 0.086 Å for **1** and 0.077 Å for **2**. The five-membered ring formed by the coordination of the ligand to the metal exhibits an envelope conformation with C1 lying at 0.913(2) Å for **1** and

0.904(5) Å for **2** out of the plane of the other four atoms Pd1/Pt1, P1, P2, and C27. The distances of Pd–Br and Pt–Br *trans* to the ylidic carbon atom are slightly shorter than the corresponding distances *trans* to the phosphorus atom (Table 3). The dihedral angle between the keto group and the attached aromatic ring is 2.02(17)° for **1** and 0.9(4)° for **2**, while the dihedral angle between the aromatic rings of the biphenyl group is 23.17(19)° for **1** and 22.8(4)° for **2**. Their structure is similar to other Pd-ylide complexes, such as dichloro-(1-(((diphenylphosphino)methyl)(diphenyl)phosphonio)-2-(2-naphthyl)-2-oxoethyl)-palladium(II)<sup>37</sup> and (2-(biphenyl-4-yl)-1-(((diphenylphosphino)methyl)-(diphenyl)phosphonio)-2-oxoethyl)-(dichloro)-palladium.<sup>35</sup> A search in the Cambridge Structural Database (CSD version 5.38, May 2017 updated) indicated that there are no known Pt analogues.

The structure of **3** is similar to those of **1** and **2** despite the coordination of the ligand, resulting in the formation of a 6-membered ring. The Pd atom is in a slightly distorted square-planar environment and coordinated by two bromine atoms, one phosphorus atom, and one ylidic carbon atom. The four coordinating atoms show a slight tetrahedral distortion with a RMS deviation of 0.126 Å, while the Pd–Br *trans* distance to the ylidic carbon atom is slightly shorter than the corresponding *trans* distances to the phosphorus atom (Table 3). The dihedral angle between the keto group and the attached aromatic ring is 4.0(12)°, while the dihedral angle between the aromatic rings of the biphenyl group is 28.6(11)°. The structure of **3** is also similar to other Pd-ylide complexes, such as dichloro-(2-(4-chlorophenyl)-1-((2-(diphenylphosphino)ethyl)(diphenyl)phosphonio)-2-oxoethyl)-palladium(II) and dichloro-(1-((2-(diphenylphosphino)ethyl)(diphenyl)phosphonio)-2-(4-methoxyphenyl)-2-oxoethyl)-palladium(II).<sup>35</sup>

### Anti-proliferative effects of the compounds

To examine the *in vitro* anti-cancer efficiency of the compounds, their potency to induce cell death was determined on H1299, U87 MG, and A2780 cell lines by using the MTT method to determine the IC<sub>50</sub> values in the micromolar range (Table S5, ESI†). An IC<sub>50</sub> value is defined as the drug concentration required for killing 50% of the cells. Comparative cytotoxicity profiles of the Pd/Pt(II) complexes **1–4** for A2780, U87 MG, and H1299 cell lines are shown in Fig. 4.

As shown in Fig. 5(a) and (b), the A2780 cells were found to be more susceptible to the as-synthesized compounds than the other two human carcinoma cell lines. Compounds **1**, **2**, **3**, and **4** exhibited interesting cytotoxic activity towards the human ovarian carcinoma cell line with the IC<sub>50</sub> values of 16 ± 3.6, 19 ± 2.7, 21 ± 1.4, and 24 ± 3.7 μM, respectively. Fig. 5 shows the effects of the compounds on the morphology of the A2780

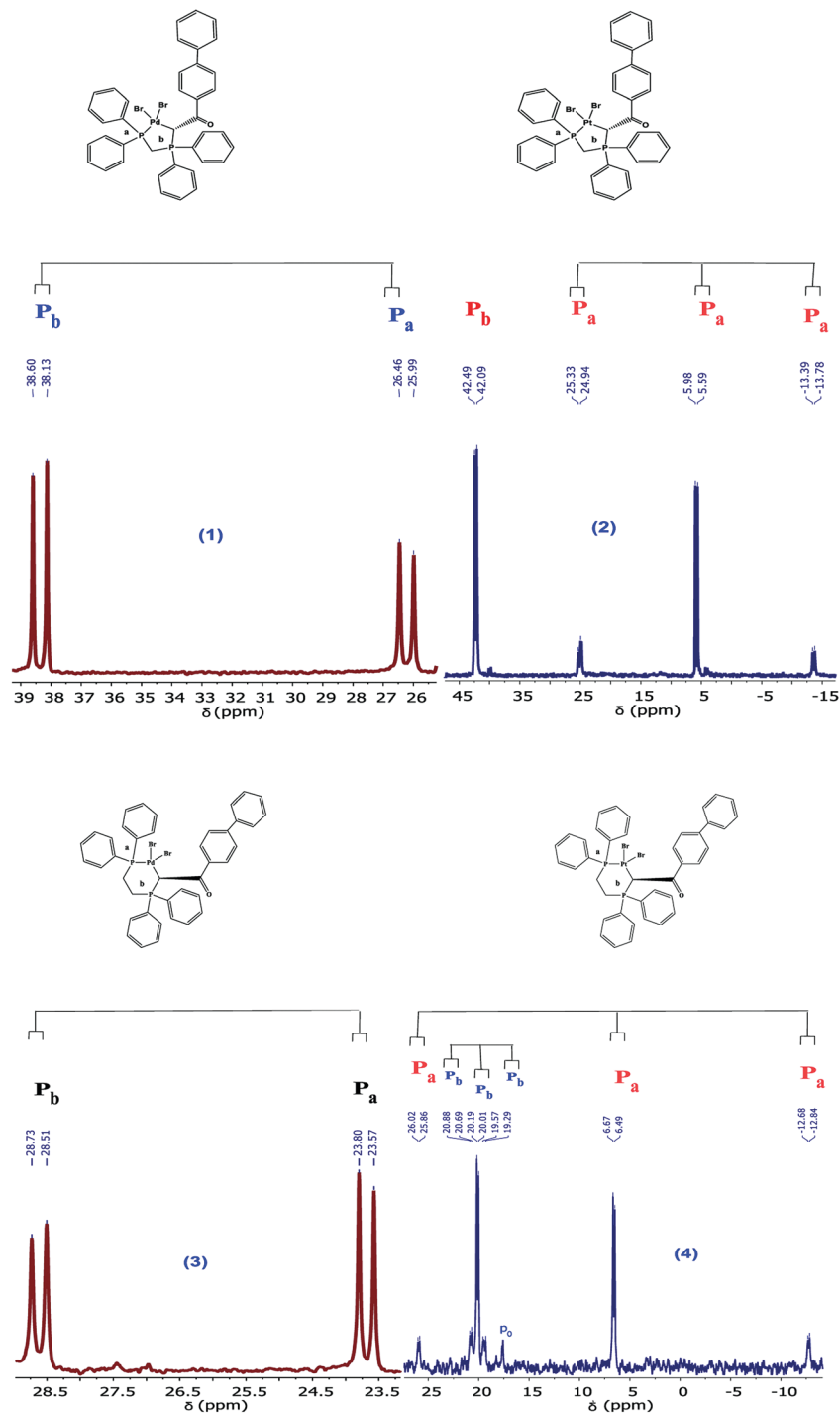


Fig. 1 The  $^{31}\text{P}$  NMR spectra of complexes **1–4**.

cells after treatment with the  $\text{IC}_{50}$  concentration of the compounds **1–4**. In our previous study, we evaluated the cytotoxicity of cisplatin, a platinum-based antineoplastic drug, in the A2780 cell line.<sup>38</sup> Our results revealed that cisplatin has a potent anti-proliferative effect against the growth of the human ovarian carcinoma cell lines ( $\text{IC}_{50} = 2.86 \mu\text{M}$ ). The cells treated with the compounds showed signs of growth inhibition, shrinkage, vacuolization, and moderate cytoplasmic granulations. Also, a

large number of treated cells became spherical and started to detach from the culture flasks. Complex **3** showed a potent anti-proliferative activity towards the human glioblastoma cell line ( $\text{IC}_{50} = 22 \pm 3.8 \mu\text{M}$ ); however, complex **4** ( $\text{IC}_{50} = 34 \pm 1.2 \mu\text{M}$ ), complex **2** ( $\text{IC}_{50} = 35 \pm 5.4 \mu\text{M}$ ), and complex **1** ( $\text{IC}_{50} = 51 \pm 7.1 \mu\text{M}$ ) displayed a moderate activity. Comparative cytotoxicity profiles of the Pd/Pt(II) complexes **1–4** for the U87 MG cells, as shown in Fig. 4, indicate the potency of the compounds as follows:

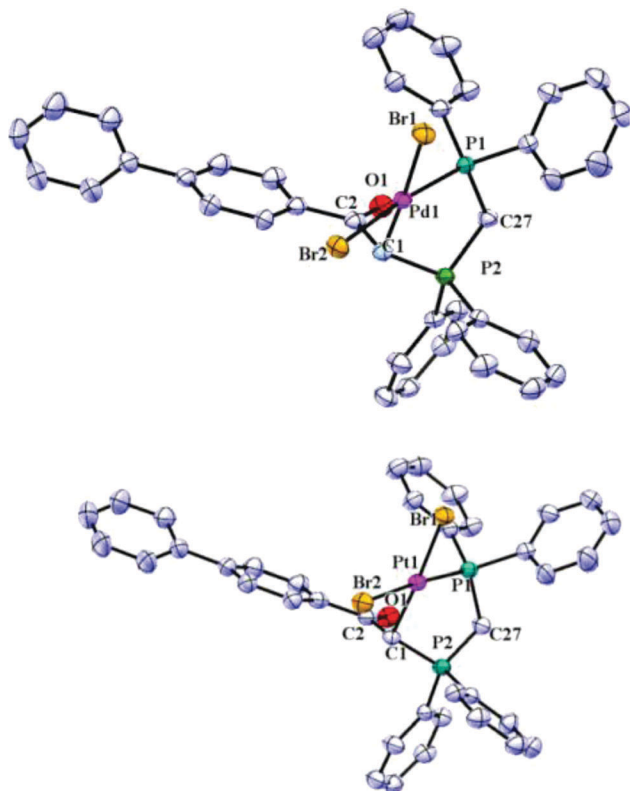


Fig. 2 ORTEP view of X-ray crystal structure of **1** and **2**.

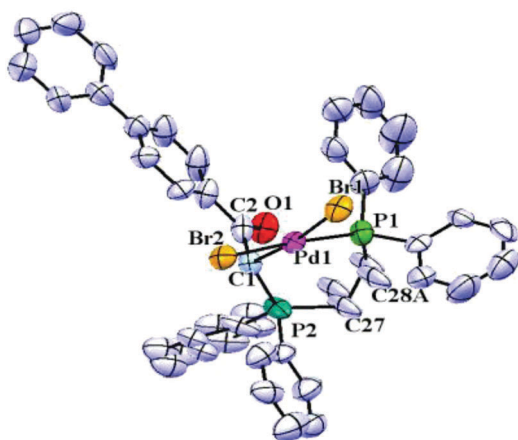


Fig. 3 ORTEP view of X-ray crystal structure of **3**.

cisplatin > **3** > **4** > **2** > **1**. Moreover, the compound **4** was able to block cell proliferation in the human non-small-cell lung carcinoma cell line H1299 ( $IC_{50} = 61 \pm 4.7 \mu\text{M}$ ), while other synthesized compounds could not inhibit cell growth at the concentration up to  $160 \mu\text{M}$ . It has been shown that increasing the dose of cisplatin reduced cell viability in the H1299 cell line and the  $IC_{50}$  values at 72 h was  $10.02 \mu\text{M}$ .

It seems that the complex **1**,  $[\text{PdBr}_2(\kappa^2\text{-Y}^1)]$ , is favorable in terms of the cytotoxic activity against the A2780 cells. Table 4 presents a comparison between the cytotoxic activities against the A2780 cell line for complex **1** and some of other Pd/Pt-based

complexes reported in the literature.<sup>39–44</sup> The results revealed that the complex **1** exhibited similar and even higher cytotoxic activity than that of the other palladium and platinum(II) complexes. Overall, based on the results of cytotoxic experiments and the comparative study, it can be concluded that the metal ions have an important effect on the anticancer activity and also, primary ligands can exert additional effects on the cytotoxicity.

### DPPH radical-scavenging activity

Free radicals are often generated as byproducts of biological reactions or from exogenous factors. The involvement of free radicals in the pathogenesis of a large number of diseases is well documented. Free radicals as potent scavengers may serve as a possible preventative interventions for diseases.<sup>45</sup> DPPH radical was used as a stable free radical to determine antioxidant activity of natural compounds.<sup>46</sup> As present, many studies focus on new antioxidant agents without harmful side effects. In the present research, free radical-scavenging capacity of the new compounds was measured by a DPPH assay and the results are shown in Table 5. Free radical-scavenging activity of **1** ( $76.08 \text{ mg mL}^{-1}$ ) was superior to those of the other samples studied. Moreover, sample **3** exerted the weakest antioxidant activity in this study ( $45.55 \text{ mg mL}^{-1}$ , Table 5) and all samples showed lower potency than ascorbic acid in scavenging of the DPPH free radical (Fig. S3, ESI†).

The higher antioxidant activity is reflected in the lower  $IC_{50}$  value. The  $IC_{50}$  value of **3** was  $0.22 \text{ (mg mL}^{-1})$ , indicating lower antioxidant activity of **3** than that of ascorbic acid; however, **1**, **2**, and **4** showed higher antioxidant activity than **3**. The radical-scavenging activity of the samples follows the order: ascorbic acid = **1** = **2** = **4** ( $IC_{50} = 0.125\text{--}0.13 \text{ mg mL}^{-1}$ ) > **3** ( $IC_{50} = 0.22 \text{ mg mL}^{-1}$ ) (Fig. 6).

### Antifungal activity

At present, most of the fungi show resistance to classical antibiotics<sup>47–50</sup> and the discovery of active compounds with novel mechanisms is a matter of urgency.<sup>51,52</sup> In agriculture, many crops of great economic importance throughout the world are host plants for *Fusarium* species causing soil-borne diseases. *F. oxysporum* is one of the soil-borne pathogens that cause severe losses of the crop of the plants of great economic importance.<sup>53,54</sup> Thus, the inhibition zone of the new compounds was determined against *F. oxysporum* (Table 6). It was observed that DMSO as a negative control had no activity against *F. oxysporum*, but the tested samples represented excellent antifungal activity that decreased with a decrease in their concentration. Moreover, **1** and **2** exerted excellent antifungal activity at the concentrations of 200 and 100 ppm, respectively (Fig. S4, ESI†). Most of the old synthetic fungicides usually degrade with great difficulty and are toxic to humans. Hence, the examined samples may be used to treat the plant diseases caused by *F. oxysporum* and also to increase resistance in a wide variety of crop plants.

### Electrochemical studies

The electrochemical behavior of free ylide (Y) and its Pd(II) complexes **1** and **2** were analyzed under the same conditions by

Table 2 Crystal data and structural refinement for **1**, **2**, and **3**

Empirical formula	C <sub>33</sub> H <sub>27</sub> C <sub>12</sub> BrOP <sub>2</sub> Pd	C <sub>39</sub> H <sub>32</sub> Br <sub>2</sub> OP <sub>2</sub> Pt	C <sub>40</sub> H <sub>34</sub> Br <sub>2</sub> OP <sub>2</sub> Pd
Formula weight	844.80	933.49	858.83
<i>T</i> [K]	130.00(10)	100.00(2)	130.01(10)
Crystal system	Orthorhombic	Orthorhombic	Orthorhombic
Space group	<i>Pbca</i>	<i>Pbca</i>	<i>Pbca</i>
<i>a</i> [Å]	14.84001(10)	14.89000(3)	15.45900(2)
<i>b</i> [Å]	16.55137(8)	16.58200(3)	16.81100(2)
<i>c</i> [Å]	28.2482(2)	28.1030(6)	27.3270(4)
$\alpha$ [°]	90	90	90
$\beta$ [°]	90	90	90
$\gamma$ [°]	90	90	90
<i>V</i> [Å <sup>3</sup> ]	6938.40(8)	6939.00(2)	7101.80(16)
<i>Z</i>	8	8	8
<i>D</i> <sub>c</sub> [Mg m <sup>-3</sup> ]	1.617	1.787	1.606
$\mu$ [mm <sup>-1</sup> ]	8.116	6.470	7.940
<i>F</i> (000)	3360.0	3616.0	3424.0
Radiation	CuK $\alpha$	Synchrotron	CuK $\alpha$
$\lambda$ (Mo-K $\alpha$ )	0.71073	0.71090	1.54184
<i>2</i> $\theta$ range [°]	8.594–154.320	2.90–63.87	8.418–136.472
Index ranges	–18 ≤ <i>h</i> ≤ 18, –13 ≤ <i>k</i> ≤ 20, –35 ≤ <i>l</i> ≤ 35	–21 ≤ <i>h</i> ≤ 21, –24 ≤ <i>k</i> ≤ 24, –41 ≤ <i>l</i> ≤ 41	–18 ≤ <i>h</i> ≤ 18, –15 ≤ <i>k</i> ≤ 20, –29 ≤ <i>l</i> ≤ 32
Refl. collected	77 741	249 011	23 200
Independent reflections	7332 [ <i>R</i> <sub>int</sub> = 0.0517]	11 006 [ <i>R</i> <sub>int</sub> = 0.0713]	6498 [ <i>R</i> <sub>int</sub> = 0.1035]
Data/restr./param.	7332/6/406	11 006/6/407	6498/96/432
Goodness-of-fit on <i>F</i> <sup>2</sup>	1.073	1.108	1.062
<i>wR</i> <sub>2</sub> [all data]	0.0698	0.1272	0.1547

Table 3 Selected bond lengths [Å] and bond angles [°] for **1**, **2**, and **3**

	<b>1</b>	<b>2</b>	<b>3</b>
Bond distances			
Pd <sub>1</sub> –Br <sub>1</sub>	2.4647(3)	2.4734(6)	2.4670(2)
Pd <sub>1</sub> –Br <sub>2</sub>	2.4882(3)	2.4876(7)	2.5124(19)
Pd <sub>1</sub> –P <sub>1</sub>	2.2305(6)	2.2109(14)	2.2400(4)
Pd <sub>1</sub> –C <sub>1</sub>	2.1050(2)	2.0980(5)	2.1100(14)
O <sub>1</sub> –C <sub>2</sub>	1.2320(3)	1.2290(7)	1.2330(19)
C <sub>1</sub> –C <sub>2</sub>	1.5030(3)	1.5010(8)	1.4700(2)
P <sub>2</sub> –C <sub>1</sub>	1.7840(2)	1.7930(5)	1.8120(15)
P <sub>1</sub> –C <sub>27</sub>	1.8650(2)	1.8700(6)	—
Bond angles			
Br <sub>2</sub> –Pd <sub>1</sub> –Br <sub>1</sub>	90.589(10)	89.190(2)	88.800(7)
C <sub>1</sub> –Pd <sub>1</sub> –P <sub>1</sub>	86.880(6)	87.820(15)	93.600(4)
C <sub>1</sub> –Pd <sub>1</sub> –Br <sub>2</sub>	90.770(6)	90.150(14)	89.900(4)
P <sub>1</sub> –Pd <sub>1</sub> –Br <sub>1</sub>	92.077(17)	93.090(4)	88.390(12)
P <sub>1</sub> –Pd <sub>1</sub> –Br <sub>2</sub>	174.571(17)	174.980(4)	173.920(14)

cyclic voltammetry at the surface of a platinum electrode in acetonitrile containing 0.1 M tetra-*n*-butylammonium perchlorate (Bu<sub>4</sub>NClO<sub>4</sub>) as the supporting electrolyte. Fig. 7I (curve a) shows the cyclic voltammogram obtained for 1 mM free ylide (Y), which shows one cathodic peak (C<sub>L1</sub>) at –0.89 V and one anodic peak (A<sub>L1</sub>) at –0.51 V vs. Ag/AgCl. Furthermore, the cyclic voltammogram of 1 mM solution of the Pd(II) complex **1** (Fig. 7I curve b) under the same conditions shows two well-defined cathodic peaks: C<sub>L1</sub> and C<sub>M1</sub>. The irreversibility of the reduction peak C<sub>M1</sub> may be related to the instability of the Pd(0) complex and its reaction with adventitious O<sub>2</sub> or other components present in the solution (chemical reaction).<sup>55,56</sup> The presence of the cathodic peak C<sub>M1</sub> in addition to the cathodic peak C<sub>L1</sub> confirms the presence of Pd(II) in the complex structure. Another interesting aspect of the comparison between curves a and b is the slight difference in the peak potentials of ligand moiety in the complex and free ligand Y.

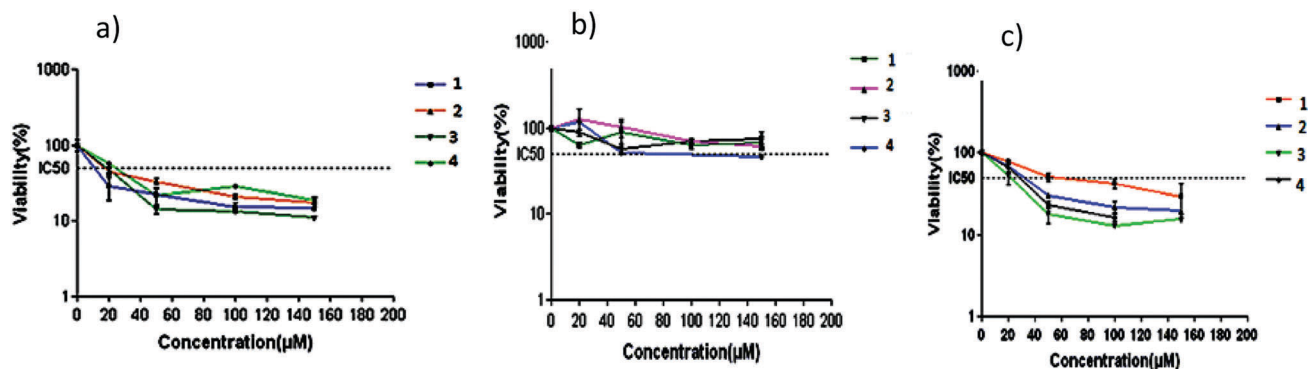


Fig. 4 Comparative cytotoxicity profiles of the Pd/Pt(II) complexes **1–4** for (a) A2780, (b) U87 MG, and (c) H1299 cell lines. The cells were incubated with different concentrations of selected compounds for 24 h. The cell proliferation inhibition was determined by the MTT assay as described in “Materials and methods”. Data are presented as mean ± S.E.M. (*n* = 3).

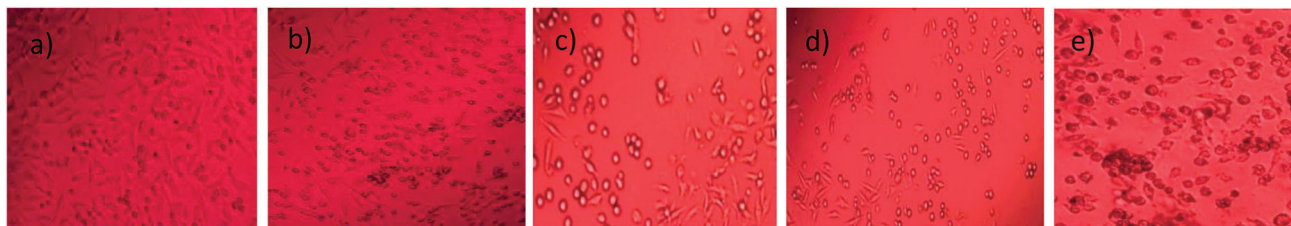


Fig. 5 Representative photomicrograph shows morphological changes of the A2780 cells. Cells were treated with (a) DMSO (control), (b) **1**, (c) **2**, (d) **3** and (e) **4** then imaged by inverted phase contrast microscope.

Table 4 Comparison of cytotoxic effects against A2780 cell line between the complex **1** and other complexes reported in the literature

Entry	Compound	IC <sub>50</sub> (μM)	Ref.
1	[Pt(terpy)] <sub>2</sub> (4,4'-trimethylenedipyridine)] (OTf) <sub>4</sub> ·H <sub>2</sub> O <sup>a</sup>	46.3	39
2	[PdL <sup>2</sup> ] [L = 2,6-diacetylpyridine bis(4 <i>N</i> -tolylthiosemicarbazonato)]	21.0	40
3	[ <i>trans</i> -PdL <sub>2</sub> Cl <sub>2</sub> ] [L = 2-methylpyridine]	34.7	41
4	[Pt <sub>2</sub> - <i>N,N'</i> -bis(2-dimethylaminoethyl oxamide)Cl <sub>4</sub> ]	53.0	42
5	[Pt(dmba)Cl (HL = a substituted 2,5-dihydro-5-oxo-1 <i>H</i> -pyrazolone-1-carbothioamide)] <sup>b</sup>	16.0	43
6	[PtL <sub>2</sub> <sup>2</sup> ] [L = thiosemicarbazone]	8.1	44
7	[PdBr <sub>2</sub> (κ <sup>2</sup> -Y <sup>1</sup> )]	16.0	This work

<sup>a</sup> terpy = 2,2':6',2''-terpyridine. <sup>b</sup> dmba = *N,N*-dimethylbenzylamine.

Table 5 DPPH radical scavenging activity (%) of new compounds and ascorbic acid

Compound	Concentration (mg mL <sup>-1</sup> )					Average
	0.2	0.4	0.6	0.8	1.0	
<b>1</b>	75.08 <sup>b</sup> ± 1.30	75.09 <sup>b</sup> ± 0.16	75.23 <sup>b</sup> ± 0.19	77.02 <sup>a</sup> ± 0.60	77.98 <sup>a</sup> ± 0.06	76.08
<b>2</b>	72.10 <sup>b</sup> ± 0.33	70.30 <sup>c</sup> ± 0.07	70.66 <sup>c</sup> ± 0.07	75.39 <sup>a</sup> ± 0.07	75.31 <sup>a</sup> ± 0.07	72.75
<b>3</b>	45.13 <sup>b</sup> ± 0.65	45.23 <sup>b</sup> ± 0.17	45.66 <sup>b</sup> ± 1.80	45.43 <sup>b</sup> ± 0.24	46.30 <sup>a</sup> ± 0.55	45.55
<b>4</b>	72.65 <sup>c</sup> ± 0.21	72.48 <sup>c</sup> ± 0.31	72.33 <sup>c</sup> ± 0.24	73.54 <sup>b</sup> ± 0.21	78.12 <sup>a</sup> ± 0.21	73.82
Ascorbic acid	80.84 <sup>a</sup> ± 0.80	81.84 <sup>a</sup> ± 1.70	81.21 <sup>a</sup> ± 1.40	80.80 <sup>a</sup> ± 2.30	80.16 <sup>a</sup> ± 1.90	80.61

The experiment was performed in triplicate and expressed as mean ± SD. The values in each row with different superscripts are significantly different ( $p < 0.05$ ).

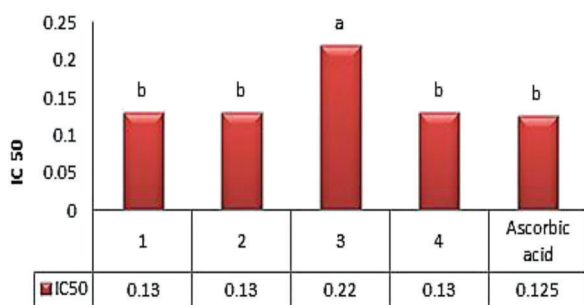


Fig. 6 Antioxidant activity (IC<sub>50</sub> value) of the new compounds and ascorbic acid. Values with different superscripts are significantly different ( $p < 0.05$ ).

The cathodic peak potential of the ligand moiety in the complex ( $E_{\text{PCL1}}^{\text{Comp}} = -1.10$  V vs. Ag/AgCl) is more negative than that of the free ligand ( $E_{\text{PCL1}}^{\text{L}} = -0.89$  V vs. Ag/AgCl). The attachment of the ligand to Pd(II) increases the reduction potential of ligand Y. Furthermore, in order to determine the exact location of two cathodic peaks C<sub>L1</sub> and C<sub>M1</sub>, we conducted another test. Fig. 7II curve c shows the cyclic voltammogram of 1 mM solution of the Pd(II) complex **1** at a scan rate of 50 mV s<sup>-1</sup>. Fig. 7II curve d is

the cyclic voltammogram of 1 mM solution of the Pd(II) complex **1** in the presence of additional amounts of free ligand Y. It can be seen that after the addition of increasing amounts of the free ligand Y, the height of the cathodic peak C<sub>L1</sub> increases significantly. This result shows that the first cathodic peak is related to the free ligand Y.

## Experimental

### Materials and methods

All synthetic reactions were carried out under dry nitrogen using standard Schlenk techniques. The chemicals 2-bromo-4'-phenylacetophenone, dppe, and dppm were purchased from commercial sources and used without further purification. [Pd/PtBr<sub>2</sub>(Cod)] was prepared according to the published procedures.<sup>57</sup> Phosphorus ylides Y<sup>1</sup> and Y<sup>2</sup> were synthesized and characterized previously.<sup>34,35</sup> The <sup>1</sup>H, <sup>13</sup>C, and <sup>31</sup>P NMR spectra were recorded at 25 °C on 250 MHz Bruker and 90 MHz Jeol spectrometers with CDCl<sub>3</sub> as the solvent. The IR spectra were recorded using KBr pellets on a Shimadzu 435-U 04 spectrophotometer in the region of 4000–400 cm<sup>-1</sup>. Cyclic voltammetric

Table 6 Antifungal activity (%) of the new compounds

Concentration (ppm)	Sample				
	1	2	3	4	DMSO
200	91.00 <sup>a</sup> ± 0.33	59.00 <sup>d</sup> ± 1.70	82.00 <sup>b</sup> ± 0.30	74.00 <sup>c</sup> ± 1.50	Na
100	21.00 <sup>c</sup> ± 0.44	44.00 <sup>a</sup> ± 3.20	10.00 <sup>d</sup> ± 1.70	28.00 <sup>b</sup> ± 1.88	Na

The experiment was performed in triplicate and expressed as mean ± SD. Values in each row with different superscripts are significantly different ( $p < 0.05$ ). Na: no active.

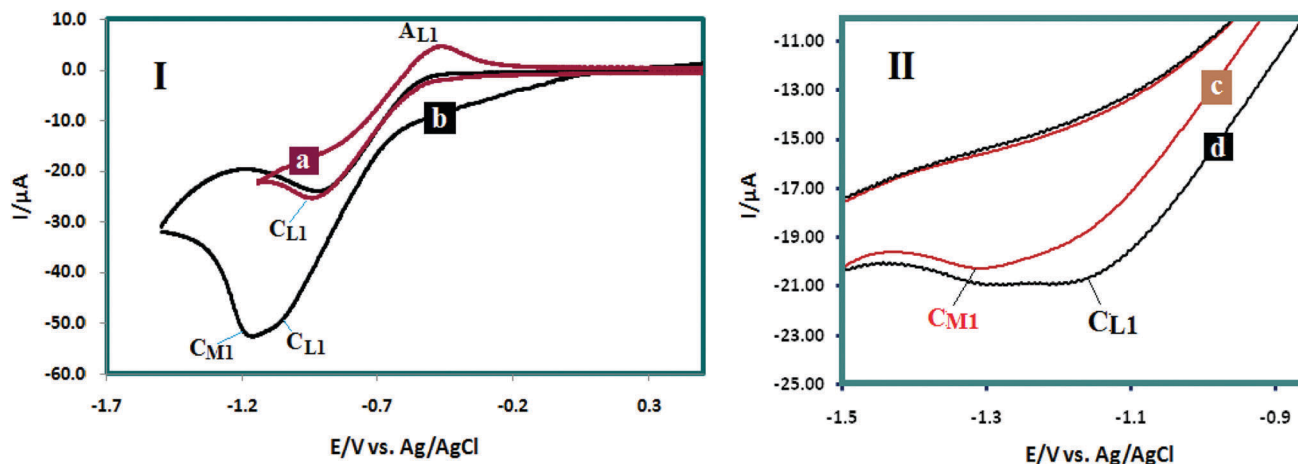


Fig. 7 (i) Cyclic voltammogram of a solution of 1 mM (a) Y and (b) 1 mM of the Pd(II) complex **1** in acetonitrile containing 0.1 M tetra-*n*-butylammonium perchlorate ( $\text{Bu}_4\text{NClO}_4$ ) as a supporting electrolyte, at the Pt electrode. Scan rate:  $100 \text{ mV s}^{-1}$ ,  $t = 25^\circ\text{C}$ . (ii) Cyclic voltammogram of a solution of 1 mM (c) 1 mM of the Pd(II) complex **1** and (d) 1 mM of the Pd(II) complex **1** in the presence of additional amounts of ligand Y in the same condition as (i) but at a scan rate of  $50 \text{ mV s}^{-1}$ .

experiments were carried out using an Autolab model PGSTAT 20 potentiostat/galvanostat. Data were recorded using a Pt disc (2.2 mm diameter), a platinum counter electrode, and an  $\text{Ag}/\text{Ag}^+$  reference electrode (all electrodes from AZAR electrodes).

### Crystallography

Single crystals of **1** ( $\text{C}_{39}\text{H}_{32}\text{Br}_2\text{OP}_2\text{Pd}$ ), **2** ( $\text{C}_{39}\text{H}_{32}\text{Br}_2\text{OP}_2\text{Pt}$ ), and **3** ( $\text{C}_{40}\text{H}_{34}\text{Br}_2\text{OP}_2\text{Pd}$ ) were crystallized by slow evaporation of their dichloromethane solution. For **1** and **3**, a suitable crystal was selected and mounted on a Rigaku Oxford Diffraction SuperNova diffractometer equipped with dual wavelength source,  $\text{CuK}\alpha$  radiation, and Atlas detector. The crystal was kept at 130 K during data collection. Data collection and reduction was carried out using CrysAlisPro with the data for both structures being corrected for absorption using Gaussian integration. Since crystals of **3** were disordered, the attempts to carry out twin processing were not successful. Crystals of **2** were small and weakly scattered and thus, data collection was carried out at 100 K at the MX1 beamline at the Australian Synchrotron and fitted with a silicon double crystal monochromator. The wavelength was tuned to approximate that of  $\text{Mo-K}\alpha$  radiation ( $\lambda = 0.7109 \text{ \AA}$ ). Data reduction was performed with XDS using strong multi-scan absorption correction in SADABS.

Using Olex2,<sup>58</sup> all three structures were solved with the ShelXT<sup>59</sup> structure solution program using Intrinsic Phasing and refined with the ShelXL<sup>60</sup> refinement package using least squares minimization. All non-hydrogen atoms were refined

with anisotropic displacement parameters, while all hydrogen atoms were placed at geometrical estimates and refined using the riding model with an isotropic displacement parameter 1.5 times (Me) or 1.2 times (other) the parent carbon atom. For **3**, one of the phenyl rings was modelled as it was being disordered over two orientations, while the atoms of the ethylene group linking the two phosphorus atoms were each distributed over two positions. The P-C and C-C distances were restrained to near ideal geometry. Since there were several residual electron density peaks of around  $2\text{--}3 \text{ e \AA}^{-3}$  close to the Pd and Br atoms, the attempts to model this disorder were not successful.

### Synthesis of the Pd/Pt complexes

**General procedure.** To a dichloromethane solution of  $[\text{MBr}_2(\text{cod})]$  ( $\text{M} = \text{Pd}$  or  $\text{Pt}$ ) (0.5 mmol, 5 mL), a solution of ylide (0.5 mmol) (5 mL,  $\text{CH}_2\text{Cl}_2$ ) was added. The resultant solution was stirred for 2 h at room temperature and then concentrated to a *ca.* 2 mL under reduced pressure and treated with *n*-hexane (5 mL) to afford the Pd/Pt(II) complexes of the desired diphosphine ylides.

**Data for  $[\text{PdBr}_2(\kappa^2\text{-Y}^1)]$  (**1**).** Yield: 0.055 g (80%), M.p.  $198\text{--}201^\circ\text{C}$ . IR (KBr disk)  $\nu(\text{cm}^{-1})$ : 1601(C=O).  $^1\text{H NMR}$  ( $\text{CDCl}_3$ )  $\delta_{\text{H}}$  (ppm): 3.7 (m,  $\text{PCH}_2\text{P}$ , 2H), 6.3 (s, 1H, PCH), 6.3–7.9 (m, 29H, Ph).  $^{31}\text{P NMR}$  ( $\text{CDCl}_3$ )  $\delta_{\text{P}}$  (ppm): 26.2 (d,  $\text{PPh}_2$ ,  $^1J_{\text{P-P}} = 46.46 \text{ Hz}$ ), 38.4 (d, PCH,  $^2J_{\text{P-P}} = 46.46 \text{ Hz}$ ).  $^{13}\text{C NMR}$  ( $\text{CDCl}_3$ , ppm)  $\delta_{\text{C}}$  (ppm): 35.4 (d,  $\text{CH}_2$ ,  $^1J_{\text{P-C}} = 72.5 \text{ Hz}$ ); 38.7 (s, PCH); 121.6–131.9 (m, Ph); 196.2 (s, CO).

**Data for  $[\text{Pt Br}_2(\kappa^2\text{-Y}^1)]$  (**2**).** Yield: 0.051 g (84%), M.p.  $195^\circ\text{C}$ . IR (KBr disk)  $\nu(\text{cm}^{-1})$ : 1600 (C=O).  $^1\text{H NMR}$  ( $\text{CDCl}_3$ )  $\delta_{\text{H}}$  (ppm):

4.8 (m, 2H, PCH<sub>2</sub>P); 5.8 (s, H, PCH); 7–8.6 (m, 29H, Ph). <sup>31</sup>P NMR (CDCl<sub>3</sub>) δ<sub>P</sub> (ppm): 5.9 (td, PPh<sub>2</sub>, <sup>1</sup>J<sub>Pt-P</sub> = 3950.11 Hz); 42.4 (d, PCH, <sup>2</sup>J<sub>P-P</sub> = 40.4 Hz). <sup>13</sup>C NMR (CDCl<sub>3</sub>, ppm) δ<sub>C</sub> (ppm): 31.2 (s, CH<sub>2</sub>); 38.7 (s, PCH); 120.6–133.5 (m, Ph); 195.6 (s, CO).

**Data for [Pd Br<sub>2</sub>(κ<sup>2</sup>-Y<sup>2</sup>)] (3).** Yield: 0.061 g (90%), M.p. 198–201 °C. IR (KBr disk) ν(cm<sup>-1</sup>): 1600 (C=O). <sup>1</sup>H NMR (CDCl<sub>3</sub>) δ<sub>H</sub> (ppm): 3.7 (m, 4H, PCH<sub>2</sub>P); 6.4 (s, 1H, PCH); 7.2–8.5 (m, 29H, Ph). <sup>31</sup>P NMR (CDCl<sub>3</sub>) δ<sub>P</sub> (ppm): 23.8 (d, PPh<sub>2</sub>, <sup>1</sup>J<sub>P-P</sub> = 23.23 Hz); 28.7 (d, PCH, <sup>2</sup>J<sub>P-P</sub> = 22.22 Hz). <sup>13</sup>C NMR (CDCl<sub>3</sub>, ppm) δ<sub>C</sub> (ppm): 22.9 (s, CH<sub>2</sub>); 31.2 (s, PCH); 122.2–134.6 (m, Ph); 196.2 (s, CO).

**Data for [Pt Br<sub>2</sub>(κ<sup>2</sup>-Y<sup>2</sup>)] (4).** Yield: 0.055 g (83%), M.p. 195 °C. IR (KBr disk) ν(cm<sup>-1</sup>): 1600(C=O). <sup>1</sup>H NMR (CDCl<sub>3</sub>) δ<sub>H</sub> (ppm): 3.7 (m, 4H, PCH<sub>2</sub>P); 6.5 (br, 1H, PCH); 7.3–7.9 (m, 29H, Ph). <sup>31</sup>P NMR (CDCl<sub>3</sub>) δ<sub>P</sub> (ppm): 6.6 (td, PPh<sub>2</sub>, <sup>1</sup>J<sub>Pt-P</sub> = 3924.9 Hz); 20.1 (td, PCH, <sup>2</sup>J<sub>P-P</sub> = 160.6 Hz). <sup>13</sup>C NMR (CDCl<sub>3</sub>, ppm) δ<sub>C</sub> (ppm): 20.2 (m, CH<sub>2</sub>); 22.4 (m, PCH); 122.4–136.6 (m, Ph); 195.9 (s, CO).

### Cell culture conditions

The H1299 (human non-small-cell lung carcinoma) cell line was a kind gift from Prof. G. Storm. The cells have a homozygous partial deletion of the p53 protein and lack p53 protein expression. The A2780 human ovarian cancer cell line was collected from tumor tissue of an untreated patient. U87 MG is a human primary glioblastoma cell line. It had epithelial morphology and was obtained from a stage-four 44 year-old cancer patient. The A2780 and U87 MG cell lines were obtained from Pasteur Institute (Tehran, Iran). The cells were cultured in Dulbecco's modified Eagle's medium (DMEM-F12) with fetal bovine serum containing 10% (v/v) heat-inactivated fetal bovine serum, 100 U mL<sup>-1</sup> penicillin, and 100 mg mL<sup>-1</sup> streptomycin and maintained at 37 °C in a humidified atmosphere (90%) containing 5% CO<sub>2</sub>.

### Cytotoxicity assay

Cytotoxic effects of the compounds were studied by the MTT assay. Exponentially growing mammalian cells (on 96-well plates) were exposed to different concentrations (0–200 μM) of the compounds for 24 h. Control cells were kept in medium containing 0.1% DMSO. After 24 h of incubation, the medium was removed, 0.1 mg per well of MTT was added to the cells, and the plates were further incubated at 37 °C for 3 h. The formazan crystals were solubilized in 0.1 mL of dimethyl sulfoxide and the optical density (OD<sub>570</sub>) was measured using a microplate reader (BioTek Instruments, USA). IC<sub>50</sub> values were calculated by plotting log<sub>10</sub> of the percentage of proliferation versus drug concentration. Moreover, images of the cells were taken at a 20× magnification using a Matic microscope equipped with a Leica digital camera.

### DPPH free radical-scavenging activity

In order to measure antioxidant activity, DPPH free radical-scavenging assay was used. Antioxidant compounds can donate electrons to stable DPPH free radicals and decay its purple color. This change in absorbance at 517 nm can be measured by a spectrophotometer. This test could provide information on (1) the ability of a compound to donate a hydrogen atom, (2) the

number of electrons a given molecule can donate, and (3) the mechanism of antioxidant action. In order to determine the radical-scavenging ability, the method reported by Mensor *et al.*<sup>61</sup> was used. The optical density of the test, control, and empty samples were measured compared to that of DMSO. The discoloration was plotted against the sample concentration in order to calculate the IC<sub>50</sub> value, which is the amount of the sample necessary to decrease the absorbance of DPPH by 50%.<sup>62</sup> The sample concentration providing 50% inhibition (IC<sub>50</sub>) was calculated from the graph plotting the inhibition percentage against the extract concentration. Tests were carried out in triplicate and ascorbic acid (AA) was used as a positive control.

### Antifungal activity

Antifungal activity of the new compounds was *in vitro* assessed against *Fusarium oxysporum* cultivated in PDA medium. The samples were added to the culture medium at two concentrations (100 and 200 ppm). In order to make the control groups, double distilled water and DMSO were added to the plates. After a 7 day-incubation of fungus on the culture medium containing the samples, radial growth of fungal mycelium was recorded. The following formula was used for calculating the inhibition rate (%): Inhibition rate (%) =  $(R - r/R) \times 100$ , where *R* is the radial growth of fungal mycelia on the control plate and *r* is the radial growth of fungal mycelia on the plate treated with the new substances. All data are the average of triplicate analyses.

### Statistical analysis

Statistical analysis of variance was performed using Student's *t*-test by SPSS program and *p* < 0.05 was regarded as significant. Data are expressed as means ± standard deviation.

## Conclusions

In this study, we reported new complexes comprising unsymmetrical phosphorus ylides Y<sup>1</sup> and Y<sup>2</sup> prepared by convenient synthetic methods in satisfactory yields. The structure of the products was characterized successfully by spectroscopic techniques such as <sup>1</sup>H, <sup>13</sup>C, <sup>31</sup>P NMR, IR, and X-ray analysis. The results showed that the phosphorus ylides coordinate to Pd and Pt in the P,C-chelated form, indicating that the metal is in a slightly distorted square-planar environment and coordinated by two bromine atoms, one phosphorus atom, and one ylidic carbon atom. The four coordinating atoms show slight tetrahedral distortion. Furthermore, *in vitro* cytotoxic activity of the new compounds was evaluated against a panel of cancer cell lines. These compounds show the high tumor-specific cytotoxicity against human ovarian carcinoma cell line, indicating that they can become new drug candidates for cancer chemotherapy. In conclusion, these compounds exhibited excellent biological activities and can be considered as a promising lead in cancer-treating drug discovery and development.

## Conflicts of interest

There are no conflicts to declare.

## Acknowledgements

Funding of our research from the Bu-Ali Sina University is gratefully acknowledged. Part of this research was undertaken on the MX1 beamline at the Australian Synchrotron, a part of ANSTO, Victoria, Australia.

## References

- 1 S. M. Cohen and S. J. Lippard, *Prog. Nucleic Acid Res. Mol. Biol.*, 2001, **7**, 93–130.
- 2 B. Lippert, *Biochem.*, 1999, 3–69.
- 3 B. Rosenberg, L. Vancamp, J. E. Trosko and V. H. Mansour, *Nature*, 1969, **222**, 385.
- 4 Y. Jung and S. J. Lippard, *Chem. Rev.*, 2007, **107**, 1387–1407.
- 5 N. Graf and S. J. Lippard, *Adv. Drug Delivery Rev.*, 2012, **64**, 993.
- 6 R. Erwin, B. V. Arion, K. B. Keppler and J. L. A. Pombeiro, *Inorg. Chim. Acta*, 2008, **361**, 1569.
- 7 R. N. Bose, L. Maurmann, R. J. Mishur, L. Yasui, S. Gupta, H. Hofstetter and T. Salley, *Proc. Natl. Acad. Sci. U. S. A.*, 2008, **105**, 18314.
- 8 G. Sava, G. Jaouen, E. Hillard and A. Bergamo, *Dalton Trans.*, 2012, **41**, 8226.
- 9 O. Heudi, S. Mercier-Jobard, A. Cailleux and P. Allain, *Biopharm. Drug Dispos.*, 1999, **20**, 107.
- 10 S. Ahmad, *Chem. Biodiversity*, 2010, **7**, 543–566.
- 11 A. k. Holzer, G. H. Manorek and S. B. Howell, *Mol. Pharmaceutics*, 2006, **70**, 1390.
- 12 M. Galanski, M. A. Jakupiec and B. K. Keppler, *Curr. Med. Chem.*, 2005, **12**, 2075.
- 13 S. Dhar, Z. Liu, J. Thomale, H. Dai and S. J. Lippard, *J. Am. Chem. Soc.*, 2008, **130**, 11467.
- 14 S. Dhar and S. J. Lippard, *Proc. Natl. Acad. Sci. U. S. A.*, 2009, **106**, 22199–22204.
- 15 A. A. Stavrovskaya, *Biochem.*, 2000, **65**, 95–106.
- 16 M. D. B. Haley and M. D. E. Frenkel, *Urol. Oncol.: Semin. Orig. Invest.*, 2008, **26**, 57.
- 17 S. Dhar, N. Kolishetti, S. J. Lippard and O. C. Farokhzad, *Proc. Natl. Acad. Sci. U. S. A.*, 2011, **108**, 1850.
- 18 A. Surrah and M. Kettunen, *Curr. Med. Chem.*, 2006, **13**, 1337.
- 19 J. Reedijk, *Proc. Natl. Acad. Sci. U. S. A.*, 2003, **7**, 3611–3616.
- 20 M. D. Hall and T. W. Hambley, *Coord. Chem. Rev.*, 2002, **232**, 49.
- 21 B. Evans, K. Raju, A. Calvert, S. Harland and E. Wiltshaw, *Cancer Treat. Rep.*, 1983, **67**, 997.
- 22 O. Rixe, W. Ortuzar, M. Alvarez, R. Parker, E. Reed, K. Paull and T. Fojo, *Biochem. Pharma.*, 1996, **52**, 1855.
- 23 D. W. Shen, L. M. Pouliot, M. D. Hall and M. M. Gottesman, *Pharma Rev.*, 2012, **64**, 706–721.
- 24 D. Leibold and R. Canetta, *Eur. J. Cancer*, 1998, **34**, 1522.
- 25 E. Wong and C. M. Giandomenico, *Chem. Rev.*, 1999, **99**, 2451.
- 26 N. Farrell, *Cancer Invest.*, 1993, **11**, 578.
- 27 F. K. Keter, *Univer. Wester. Cap.*, 2004, 1–123.
- 28 J. L. Butoura, S. Wimmerb, F. Wimmerb and P. Castanc, *Chem.-Biol. Interact.*, 1997, **104**, 165.
- 29 A. S. Abu-Surrah, K. A. A. Safieh, I. M. Ahmad, M. Y. Abdalla, M. T. Ayoub, A. K. Qaroush and A. M. Abu-Mahtheieh, *Eur. J. Med. Chem.*, 2010, **45**, 471.
- 30 F. Z. Wimmer, S. Wimmer, P. Castan, S. Cros, N. Johnson and E. Colacio-Rodriguez, *Anticancer Res.*, 1989, **9**, 791–794.
- 31 I. Warad, A. F. Eftaiha, M. A. Al-Nuri, A. I. Husein, M. Assal, A. Abu-Obaid, N. Al-Zaqri, T. B. Hadda and B. Hammouti, *J. Mater. Environ. Sci.*, 2013, **4**, 542–557.
- 32 G. Zhao, H. Lin, P. Yu, H. Sun, S. Zhu, X. Su and Y. Chen, *J. Inorg. Biochem.*, 1999, **73**, 145.
- 33 F. Caires and A. C. Favero, *Anti-Cancer Agents Med. Chem.*, 2007, **7**, 484.
- 34 S. J. Sabounchei, S. Samiee, S. Salehzadeha, Z. B. Nojinib and E. Irranc, *J. Organomet. Chem.*, 2010, **695**, 1441–1450.
- 35 S. J. Sabounchei, M. Panahimehr, M. Ahmadi, Z. Nasri and H. R. Khavasi, *J. Organomet. Chem.*, 2013, **723**, 207.
- 36 M. Kalyanasundari, K. Panchanatheswaran, W. T. Robinson and H. Wen, *J. Organomet. Chem.*, 1995, **491**, 103.
- 37 S. J. Sabounchei, M. Hosseinzadeh, M. Panahimehr, D. Nematollahi, H. R. Khavasi and S. Khazalpour, *Transition Met. Chem.*, 2015, **40**, 657.
- 38 B. Jamali, M. Nakhjavani, L. Hosseinzadeh, S. Amidi, N. Nikounezhad and F. H. Shirazi, *Iran. J. Pharm. Res.*, 2015, **14**, 513.
- 39 B. W. J. Harpera and J. R. Aldrich-Wright, *Dalton Trans.*, 2015, **44**, 87.
- 40 A. I. Matesanz, I. Leitao and P. Souza, *J. Inorg. Biochem.*, 2013, **125**, 26–31.
- 41 M. E. H. Mazumder, P. Beale, C. Chan, J. Q. Yu and F. Huq, *ChemMedChem*, 2012, **7**, 1–8.
- 42 L. Messori, J. Shaw, M. Camalli, P. Mura and G. Marcon, *Inorg. Chem.*, 2003, **42**, 6166–6168.
- 43 J. S. Casas, E. E. Castellano, J. Ellena, M. S. Garcia-Tasende, M. L. Perez-Paralle, A. Sanchez, A. Sanchez-Gonzalez, J. Sordo and A. Touceda, *J. Inorg. Biochem.*, 2008, **102**, 33–45.
- 44 A. Zamora, V. Rodriguez, N. Cutillas, G. S. Yellol, A. Espinosa, K. G. Samper, M. Capdevila, O. Palacios and J. Ruiz, *J. Inorg. Biochem.*, 2013, **128**, 48–56.
- 45 G. Xu, H. Yu, X. Shi, L. Sun, Q. Zhou, D. Zheng, H. Shi, N. Li, X. Zhang and N. Li, *BMC Pulm. Med.*, 2014, **14**, 174.
- 46 M. A. Gyamfi, M. Yonamine and Y. Aniya, *Gene. Pharmac. Vascul. Sys.*, 1999, **32**, 661.
- 47 M. Ozturk, F. A. Ozturk, M. E. Duru and G. Topcu, *Food Chem.*, 2007, **103**, 623.
- 48 S. A. Rice, M. Givskov, P. Steinberg and S. Kjelleberg, *J. Mol. Microbiol. Biotechnol.*, 1999, **1**, 23.
- 49 A. Ironmonger, B. Whittaker, A. J. Baron, B. Clique, C. J. Adams, A. E. Ashcroft, P. G. Stockley and A. Nelson, *Org. Biomol. Chem.*, 2007, **5**, 1081.
- 50 A. A. Hussain, A. A. Mohammed, H. H. Ibrahim and A. H. Abbas, *World Acad. Sci. Eng. Technol.*, 2009, **57**, 433.
- 51 A. A. Al-Amiery, *Med. Chem. Res.*, 2012, **21**, 3204–3213.
- 52 A. A. H. Kadhum, A. B. Mohamad, A. A. Al-Amiery and M. S. Takriff, *Molecules*, 2011, **16**, 6969.
- 53 G. N. Agrios, *Plant Pathol.*, 1988, 803.
- 54 R. P. Larkin and D. R. Fravel, *Plant Dis.*, 1998, **82**, 1022.

- 55 G. Buscemi, M. Basato, A. Biffis, A. Gennaro, A. A. Isse, M. M. Natile and C. Tubaro, *J. Organomet. Chem.*, 2010, **695**, 2359.
- 56 A. J. Downard, A. M. Bond, A. J. Clayton, L. R. Hanton and D. A. McMorran, *Inorg. Chem.*, 1996, **35**, 7684.
- 57 D. Drew, J. R. Doyle and A. G. Shaver, *Inorg. Synth.*, 1972, **13**, 47.
- 58 O. V. Dolomanov, L. J. Bourhis, R. W. Grosse-Kunstleve, P. D. Adams, R. J. Gildea, J. A. K. Howard and H. Puschmann, *J. Appl. Crystallogr.*, 2011, **44**, 1259–1263.
- 59 G. M. Sheldrick, *Acta Crystallogr., Sect. C: Struct. Chem.*, 2015, **C71**, 3–8.
- 60 G. M. Sheldrick, *Acta Crystallogr., Sect. A: Cryst. Phys., Diffraction, Theor. Gen. Crystallogr.*, 2015, **A71**, 3–8.
- 61 L. L. Mensor, F. S. Menezes, G. G. Leitao, A. S. Reis, T. S. Santos and C. S. Coube, *Phytother. Res.*, 2001, **15**, 127.
- 62 I. I. Koleva, T. A. V. Beek, J. P. H. Linssen, A. D. Groot and L. N. Evstatieva, *Phytochem. Anal.*, 2002, **13**, 8.